Automatic Segmentation of the Spinal Cord and the Dural Sac in Lumbar MR Images Using Gradient Vector Flow Field

Jaehan Koh, Taehyong Kim, Vipin Chaudhary, and Gurmeet Dhillon

Abstract— **A Computer-aided diagnosis (CAD) system aims to facilitate characterization and quantification of abnormalities as well as minimize interpretation errors caused by tedious tasks of image screening and radiologic diagnosis. The system usually consists of segmentation, feature extraction and diagnosis, and segmentation significantly affects the diagnostic performance. In this paper, we propose an automatic segmentation method that extracts the spinal cord and the dural sac from T2-weighted sagittal magnetic resonance (MR) images of lumbar spine without the need of any human intervention. Our method utilizes a gradient vector flow (GVF) field to find the candidate blobs and performs a connected component analysis for the final segmentation. MR Images from fifty two subjects were employed for our experiments and the segmentation results were quantitatively compared against reference segmentation by two medical specialists in terms of a mutual overlap metric. The experimental results showed that, on average, our method achieved a similarity index of 0.7 with a standard deviation of 0.0571 that indicated a substantial agreement. We plan to apply this segmentation method to computer-aided diagnosis of many lumbar-related pathologies.**

I. INTRODUCTION

Computer-aided diagnosis (CAD) aims at assisting medical doctors in their diagnostic decision-making processes. Even though the final diagnosis should be made by the doctor, a CAD system has been widely utilized based on a variety of modalities such as X-ray, ultrasound, computed tomography (CT), and magnetic resonance imaging (MRI), assisting physicians in their early detection of various abnormalities such as breast cancers, lung nodules, vertebral fractures, and intracranial aneurysms [1]. A CAD system consisting of segmentation, feature extraction and diagnosis, usually aims to facilitate characterization and quantification of abnormalities as well as minimize interpretation errors caused by tedious tasks of image screening and radiologic diagnosis. The interpretation is affected by the skills and the experience of the radiologist as well. Thus, by providing the radiologist with a second opinion by a computer, the time needed for accurate diagnosis can be reduced and interpretation can be enhanced minimizing errors. Accordingly, as imaging technology and computation capability advance, it is expected that CAD systems will be incorporated into Picture Archiving and Communication Systems and be used daily for diagnostic examinations in many clinical settings [1].

The spinal cord is a crucial communication channel between brain and body that constitutes the central nervous system (CNS). This cylindrical structure of nervous tissues is clinically important since it can develop several diseases including tumors and inflammations that may result in paralysis. It is known that the following common diseases related to the spinal cord are captured in MRI: tumors, infections, syringohydromyelia, spinal cord trauma, vascular malfunction, inflammatory and degenerative diseases [2] [3]. In a lateral view, the spinal cord reaches around the level $L2$ and the dural sac shielding the spinal cord terminates around the level $S2$. In MR images, the spinal cord may be used as a landmark region that helps locate a region of interest (ROI) and locate neighboring vertebra and intervertebral discs because of its high brightness as well as relatively homogeneous texture patterns.

Since ROI segmentation is a preprocessing step to feature extraction and computational diagnosis in the CAD system, in this paper we propose an automatic GVF field-based segmentation method that extracts the spinal cord and the dural sac in T2-weighted sagittal MR images of lumbar spine. In our experiments, MR images obtained by T2-weighted sagittal protocol are chosen since they are typically viewed in clinical environments for a primary examination. Experimental results on the 52 subjects are compared against reference segmentation by two medical specialists and validated through a supervised evaluation.

A. Related Work

It is reported that many research groups have focused on segmentation of the spinal cord and the spinal canal in CT. Karangelis and Zimeras [4] introduced a semi-automatic three-dimensional method for segmenting the spinal cord from CT images. On each slice level, they used a boundary tracking method along with linear interpolation in the $z-$direction. However, the proper selection of the location of the seed point and the threshold limited its applicability. Archip *et al.* [5] presented a top-down knowledge-based technique that identified the spinal cord in CT images. This approach used an anatomical structures map (ASM) and a

J. Koh is with the Department of Computer Science and Engineering, University at Buffalo (SUNY), Buffalo, NY 14260, USA jkoh@buffalo.edu

T. Kim is with the Department of Computer Science and Engineering, University at Buffalo (SUNY), Buffalo, NY 14260, USA thkim7@buffalo.edu

V. Chaudhary is with Faculty of the Department of Computer Science and Engineering, University at Buffalo (SUNY), Buffalo, NY 14260, USA vipin@buffalo.edu

G. Dhillon is with Proscan Imaging of Buffalo, Williamsville, NY 14221, USA gdhillon@proscan.com

* The research was supported in part by a grant from NYSTAR and NSF.

task-oriented architecture plan solver. The authors argued that the method was flexible enough to handle inter-patient variation and transparent to the radiologist ensuring that the experts can take control of undesirable results by image analysis. However, it required a high computational cost and sometimes the user needed to manually correct the errors. Burnett *et al.* [6] developed a semi-automatic algorithm for spinal canal segmentation of CT images. The spinal canal was partially delineated by wavelet-based edge detection and fitted to a deformable model. Later, the template was aligned manually to fit more accurately to the spinal canal. The performance of the algorithm was assessed by comparison with contours generated manually by radiation oncologists. Nyúl *et al.* [7] proposed a semi-automatic segmentation method that extracted the spinal cord/canal from CT images. An initial seed point set by a human allowed to perform region-growing and active contour techniques automatically. This method was validated by comparison with standard reference.

In addition, many MRI-based approaches have been reported recently. Nieniewski and Seneels [8] proposed a morphological method to segment the spinal cord from MR images. After correcting the image by the white top hat transform with a large structuring element, the gray matter was extracted in a semi-automatic way. The method was tested on images from cross-sections of the spinal cord. In this method, a user was required to provide the first region for it to determine subsequent regions. Coulon *et al.* [9] proposed a semi-automatic method for segmenting and visualizing the surface of the spinal cord from the MRI based on the optimization of a B-spline active surface model. The method was applied to atrophy detection via measuring the cross-sectional area along the cord. Schmit and Cole [10] proposed a semi-automatic method for segmentation of the spinal cord and injury diagnosis. Based on initial seed points that were provided manually on each data set, a three-dimensional seeded region growing technique was used. By comparing the neurologically and spinal cord injured subjects in terms of MRI segmented areas, they localized the problematic area and assessed the injury level. Uitert *et al.* [11] presented a semi-automatic process for segmenting the spinal cord from MRI and for determining the total length and the area between adjacent pairs of intervertebral discs. After seed points were given along the center of the spinal cord, the centerline of the spinal cord was determined. Then, a smoothed centerline by a Gaussian filter was used to partition the spinal cord region. McIntosh and Hamarneh [12] presented a semi-automatic spinal cord segmentation and analysis technique from MRI using high-level, autonomically-driven control mechanisms. In their method, segmentation was done based on geometrical, physical, sensory, cognitive, and behavioral layers. The model was quantitatively validated and compared against a manual segmentation method that used the connected components and ITK-SNAP's level-set method. However, this method took 10 minutes per image on average

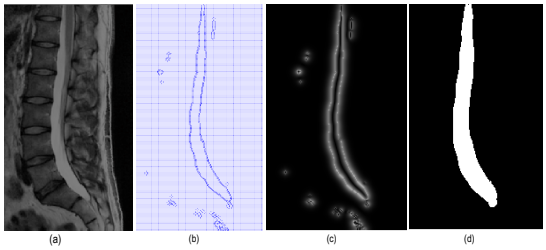

Fig. 1. Input image and intermeidate results. (a) shows the input sagittal image, (b) shows the GVF edge map, (c) represents its magnitude, and (d) is the final segmented result.

and required two seed points by a user. Horsfield *et al.* [13] proposed a semi-automatic method for segmentation of the spinal cord from MRI. The model utilized an active surface model that was formed from the approximated cord centerline marked by a human and was applied to assessing the multiple sclerosis. The method was evaluated in terms of the intra-observer reproducibilities.

The methods presented above are either semi-automatic or did not report any validation. Different from them, our method works in a fully automatic way and is quantitatively validated through a mutual overlap metric. The rest of the paper is organized as follows. In Section 2, our automatic segmentation method for segmentation of the spinal cord and the dural sac is introduced. Then, experimental results and discussion are given in Section 3 and Section 4, respectively. Finally, the conclusions and future directions of research are explained in Section 5.

II. METHOD

Our segmentation is performed in three steps. In the preprocessing step, an ROI containing the spinal cord and the dural sac is extracted. A gradient vector flow (GVF) edge map and its magnitude are computed in the second step. In the post-processing step, holes in the connected components generated by thresholding the the map are filled and small blobs likely to be noise are eliminated.

A. Preprocessing

In this step, the mid-sagittal image among a set of slice images is selected based on the slice number information stored in a Digital Imaging and Communications in Medicine (DICOM) header. It is reported that the mid-sagittal T2-weighted image gives the best contrast between the spinal canal and its adjacent structures [2]. After the middle slice is selected, an ROI containing the spinal cord is determined. Empirically, in each mid-slice, the spinal cord is contained in the middle region, between 150 pixels from the left corner and 180 pixels from the right corner. The pixels in the background regions (*i.e.*, other than the selected ROI) are marked as black to expedite subsequent image processing.

B. Gradient vector flow computation

The traditional active contour model or snake is defined as an energy-minimizing spline which gives desired image properties at their local minima of the energy functional [14]. The snake is parametrically defined as $\mathbf{v}(s) = [x(s), y(s)]$,

where $x(s), y(s)$ are $x-, y-$ coordinates along the contour and $s \in [0, 1]$. The energy functional $E(\mathcal{C})$ to be minimized is expressed as

$$E(\mathcal{C}) = \int_0^1 \frac{1}{2}\left(\alpha|\mathbf{v}'(s)|^2 + \beta|\mathbf{v}''(s)|^2\right) + E_{ext}\big(\mathbf{v}(s)\big)ds, \quad (1)$$

where α, and β specify the elasticity and stiffness of the contour, respectively, and $\mathbf{v}'(s)$ and $\mathbf{v}''(s)$ are the first and second derivatives of $\mathbf{v}$ with respect to s. The external energy term E_{ext} determines the constraints of contour evolution depending on the image $I(x, y)$. The Euler-Lagrange condition states that the spline $\mathbf{v}(s)$ must satisfy the following condition to minimize $E(\mathcal{C})$

$$\alpha\mathbf{v}''(s) - \beta\mathbf{v}''''(s) - \nabla E_{ext} = \mathbf{0}. \quad (2)$$

This can be regarded as a force balance equation

$$\mathbf{F}_{int} + \mathbf{F}_{ext}^{(1)} = \mathbf{0}, \quad (3)$$

where $\mathbf{F}_{int} = \alpha\mathbf{v}''(s) - \beta\mathbf{v}''''(s)$ and $\mathbf{F}_{ext}^{(1)} = -\nabla E_{ext}$. The external forces computed from the variational equation (1) must satisfy the force balance equation (2) as a static irrotational field [15].

GVF field is invented as a non-irrotational external force field that points toward the boundary of the object when in their proximity and varies smoothly over homogeneous image regions heading towards image borders. Formally, the GVF field is defined to be the vector field $\mathbf{g} = (x, y) = \big(u(x, y), v(x, y)\big)$ that minimizes the energy functional

$$E = \int\int \mu\big(u_x^2 + u_y^2 + v_x^2 + v_y^2\big) + |\nabla f|^2|\mathbf{g} - \nabla f|^2 dxdy, \quad (4)$$

where μ is a regularization parameter balancing the weight of the first and second terms and the subscripts denote directional partial derivatives. If $|\nabla f|$ is small, the energy functional is dominated by partial derivatives of the vector field. On the other hand, if $|\nabla f|$ is large, the energy functional is dominated by the second term. In this equation, a parameter μ regulates the trade-off between the first and the second term.

According to variational calculus, the GVF can be obtained by solving the decoupled Euler equations

$$\mu\nabla^2 u - (u - f_x)(f_x^2 + f_y^2) = 0, \quad (5)$$

$$\mu\nabla^2 v - (v - f_y)(f_x^2 + f_y^2) = 0, \quad (6)$$

where ∇^2 is a Laplacian operator. The equations (5) and (6) can be solved as separate scalar partial differential equations in u and v.

Once the GVF field is computed, the magnitude of each pixel $M(x, y)$ is computed by

$$M(x, y) = \big|\sqrt{\nabla \mathbf{g}}\big|. \quad (7)$$

C. Post-processing

In this step, connected components are filled and small components are removed. After an edge map is generated and its magnitude is thresholded, all holes within each connected component are filled based on 8-connected neighbors. Then, the blobs that are less likely to be part of the spinal canal are eliminated by a connected component analysis. That is, small components are removed based on the number of elements in each class. For each class, a membership value is assigned to each pixel and the number of elements in each connected component is computed. The component that has the largest number of elements is firstly classified as the spinal cord region. After this, connected components that satisfy the following condition are also classified as the spinal cord region: $0.65 \times C_L$ where C_L denotes the number of pixel elements of the largest connected component. This step includes the cord region that had been excluded in the segmentation due to intensity variation caused by disc herniation or spinal stenosis. The coefficient of 0.65 is chosen heuristically.

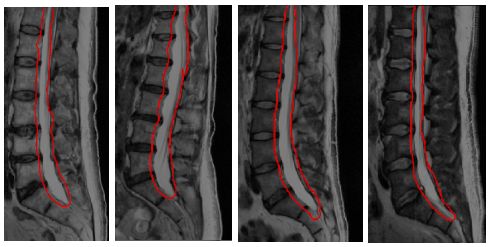

Fig. 2. Automatic segmentation results based on the GVF field.

III. EXPERIMENTS

The performance of the automatic segmentation based on the GVF field was compared with the manually marked boundaries by two trained medical specialists. The experiments were carried out on 52 subjects without any human intervention. Thus, there was no need to provide any information for segmentation of the spinal cord and the dural sac.

A. Image data and standard reference

For MRI segmentation, a total of 646 MR images from 52 subjects of ages between 28 and 84 were used. Images were taken by a 3-T Philips scanner. The imaging parameters used for the scanner were echo time of 100 *ms*, repetition time of 2622 *ms*, and slice thickness of 4.5 *mm*, and matrix dimension of 512×512 pixels. The sagittal slice direction and a flip angle of 90° were employed for all subjects.

Standard reference, *i.e.*, reference segmentation was provided as a set of $x-$ and $y-$ coordinates by two medical specialists as previously stated.

B. Automatic segmentation based on GVF field

To generate the GVF field, an edge map $f(x, y)$ should be calculated from the image $I(x, y)$ in advance. According to Xu and Prince [15] there are several choices for $f(x, y)$ and we used $f(x, y) = |\nabla I(x, y)|$ where $I(x, y)$ is the image. The regularization parameter μ of 0.1 was used for edge map generation.

The magnitude of the edge map was used to determine the contour of the spinal cord and the dural sac and it was binarized using an optimal threshold calculated by Otsu's method. After getting blobs by filling holes of the connected components, spurious spinal cord regions were eliminated on

the basis of the number of elements in each blob. Once the final segmentation result using the GVF field was obtained, it was compared against reference segmentation.

Evaluating a segmentation result usually involves the following two questions [16]: (i) How do we determine whether or not the segmented area is the right one? (ii) How do we evaluate the segmentation result objectively?

As a solution to the first question, the spinal cord regions were manually marked by two medical specialists and the boundaries of the spinal cord were used as reference segmentation, being regarded as the "right" ones. For the second one, a mutual overlap approach was adopted. The mutual overlap metric M_{SI} is based on the area of overlap between the segmented region by a computer and the standard reference by humans [17]. Specifically, the mutual overlap metric M_{SI} is defined as two times the area of the mutual overlap A_{MO} normalized by the area of reference segmentation A_R and the area of segmented region A_S, *i.e.*,

$$M_{SI} = 2 \cdot \frac{A_{MO}}{A_R + A_S}. \quad (8)$$

This measure is derived from a reliability measure known as the kappa (κ) statistic to evaluate the inter-observer agreement in regard to categorical data. According to this $M_{SI} > 0.8$ indicates perfect agreement, $0.6 < M_{SI} \leq 0.8$ represents substantial agreement, and $0.4 < M_{SI} \leq 0.6$ moderate agreement [18]. Since one of our goals for this research is to develop an automatic segmentation method that is comparable to human segmentation, we chose to employ the same metric that measures inter-observer variability.

IV. Discussion

In the experiments, spinal cord segmentation was conducted using 646 MR images from 52 patients. Given a sagittal slice as in Fig. 1(a), the GVF edge map finds the contour of the spinal cord and the dural sac accurately as in Fig. 1(b) since the intensity difference is relatively significant in this region. The magnitude of the GVF edge map is then calculated by equation (7). As we can see in Fig. 1(c), the edge map has larger vector flows near the target contour. In addition, it shows tiny flow fields in homogeneous regions in the MR image. After small connected components are removed, the final segmented result is obtained as in Fig. 1(d). Fig. 2 shows several segmentation results that localize the spinal cord region.

Table 1 evaluates the segmentation result between the output by a computer and standard reference by a specialist in terms of the mutual overlap metric. As the mean similarity index for both observers are 0.7 with a small difference in standard deviations (*i.e.*, around 1.4%), the segmented result from our method matches significantly with the reference segmentation with little fluctuation.

TABLE I

The mean and standard deviation of the similarity index between the automatic segmentation and standard reference

Metric	Observer 1	Observer 2
Mean of M_{SI}	0.70	0.70
Standard deviation of M_{SI}	0.0501	0.0641

V. Conclusions and Future Works

In this paper, we propose an automatic segmentation method that extracts the spinal cord and the dural sac in T2-weighted sagittal MR images of lumbar spine. For segmentation, a gradient vector flow field is employed, followed by a connected component analysis. MR Images taken from fifty two subjects are employed and the segmentation results are quantitatively compared against reference segmentation by two medical specialists in terms of a mutual overlap metric. The experimental results showed that our method achieved a similarity index of 0.7 with a standard deviation of 0.0571 on average that indicated a substantial agreement. In the future, we plan to apply this segmentation method to computer-aided diagnosis of many lumbar-related pathologies.

References

[1] K. Doi, "Computer-aided diagnosis in medical imaging: Historical review, current status and future potential", *in Computerized Medical Imaging and Graphics*, vol. 31, 2007, pp. 198-211.

[2] P.F. Beattie and S.P. Meyers, "Magnetic Resonance Imaging in Low Back Pain: General Principles and Clinical Issues", *Physical Therapy*, vol. 78, 1998, pp. 738-753.

[3] N.J. Sheehan, "Magnetic resonance imaging for low back pain: indications and limitations", *ARD*, vol. 69, 2010, pp. 7-11.

[4] G. Karangelis and S. Zimeras, "An Accurate 3D Segmentation Method of the Spinal Canal Applied to CT Data", *BVM*, 2002, pp. 370-373.

[5] N.A. Archip, P-J. Erard, M. Egmont-Petersen, J-M. Haefliger, and J-F. Germond, "A Knowledge-Based Approach to Automatic Detection of the Spinal Cord in CT Images", *TMI*, vol. 21, 2002, pp. 1504-1516.

[6] S.S.C. Burnett, G. Starkschall, C. W. Stevens and Z. Liao, "A deformable-model approach to semi-automatic segmentation of CT images demonstrated by application to the spinal canal", *Med. Phys.*, vol. 31, 2004, pp. 251-263.

[7] L.G. Nyúl, J. Kanyó, E. Máté, G. Makay, E. Balogh, M. Fidrich, and A. Kuba, "Method for Automatically Segmenting the Spinal Cord and Canal form 3D CT Images", *CAIP 2005*, vol. 3691, 2005, pp. 456-463.

[8] M. Nieniewski and R. Serneels, "Segmentation of Spinal Cord Images by Means of Watershed and Region Merging Together with Inhomogeneity Correction", *IJMGV*, vol. 11, 2002, pp. 101-121.

[9] O. Coulon, S.J. Hickman, G.J. Parker, G.J Barker, D.H. Miller, and S.R. Arridge, "Quantification of Spinal Cord Atrophy From Magnetic Resonance Images Via a B-Spline Active Surface Model", *Magnetic Resonance in Medicine*, vol. 47, 2002, pp. 1176-1185.

[10] B.D. Schmit and M.K. Cole, "Quantification of Morphological Changes in the Spinal Cord in Chronic Human Spinal Cord Injury using Magnetic Resonance Imaging", *EMBS*, 2004, pp. 4425-4428.

[11] R.V. Uitert, I. Bitter, and J.A. Butman, "Semi-Automatic Spinal Cord Segmentation and Quantification", *CARS*, 2005, pp. 224-229.

[12] C. McIntosh and G. Hamarneh, "Spinal Crawlers: Deformable Organisms for Spinal Cord Segmentation and Analysis", *MICCAI 2006*, vol. 4190, 2006, pp. 808-815.

[13] M.A. Horsfield, S. Sala, M. Neema, M. Absinta, A. Bakshi, M.P. Sormani, M.A. Rocca, R. Bakshi, and M. Filippi, "Rapid Semi-Automatic Segmentation of the Spinal Cord from Magnetic Resonance Images: Application in Multiple Sclerosis", *NeuroImage*, vol. 50, 2010, pp. 446-455.

[14] M. Kass, A. Witkin and D. Terzopoulos, "Snakes: Active contour models", *IJCV*, vol. 1, 1987, pp. 321-331.

[15] C. Xu and J.L. Prince, "Snakes, Shapes, and Gradient Vector Flow", *IEEE Transactions on Image Processing*, vo. 7, 1998, pp. 359-369.

[16] M. Sonka, V. Hlavac, and R. Boyle, "Image Processing, Analysis, and Machine Vision", *Thomson Learning* , 2008.

[17] S.K. Michopoulou, L. Costaridou, E. Panagiotopoulos, R. Speller, G. Panayiotakis, and A. Todd-Pokropek, "Atlas-Based Segmentation of Degenerated Lumbar Intervertebral Discs From MR Images of the Spine", *TBME*, vol. 56, 2009, pp. 2225-2231.

[18] H. L. Kundel, "Measurement of Observer Agreement", *RSNA*, 2003, pp. 303-308.